Morphodynamic changes in a channel confluence due to local tributary widening

M. Leite Ribeiro
Laboratory of Hydraulic Constructions (LCH)
Ecole Polytechnique Fédérale de Lausanne (EPFL)
Station 18, 1015 Lausanne
SWITZERLAND
E-mail: marcelo.leiteribeiro@epfl.ch

Abstract: *The morphodynamic changes in a confluence zone due to local tributary widening were experimentally investigated in a set-up representative of regulated piedmont confluences. A reference configuration with a constant tributary width of 0.15 m is compared to a configuration where the tributary is widened to 0.30 m over its last 0.45 m. The main channel is 0.5 m wide and the confluence angle is 90°. Comparison is made for a discharge ratio* $Q_t/Q_m = 0.11$*. Tests were run until equilibrium with a constant solid discharge of poorly-sorted material from the tributary. The paper presents detailed data on the morphology and on the three-dimensional flow velocity field at the confluence zone. Results revealed that the local widening of the tributary creates a pronounced heterogeneity in the flow velocities and flow depths, without having any adverse effects on flood safety in the confluence zone. Although the local tributary widening allows a reduction in the confluence angle, it locally amplifies the hydro-morpho-sedimentary processes in the confluence zone.*

Keywords: *channel confluences, experimental investigation, morphodynamics, river rehabilitation.*

1. INTRODUCTION

During the past centuries, many rivers have been channelized and regulated, often with the aim of reclaiming land for urbanization and agriculture. These river training works typically resulted in linear river systems with quasi-homogeneous flow and morphologic conditions, which reduced the natural dynamics, impoverished ecological value and promoted a deficit in flood safety. The Upper Rhone River in Switzerland (Figure 1) is an example of such a regulated river that is currently in an ecological poor state. It is mainly because of the channelization of the Rhone and its tributaries and the rupture of the lateral connectivity of the fluvial system (Bourgeois, 2006).

Although the morphodynamics of lowland channel confluences where the tributary and the main channel have similar dimensions are well documented in the literature (Best, 1987; Biron et al., 1993; Rhoads & Kenworthy, 1995; Biron et al., 1996), piedmont confluences as found in the Upper Rhone River have hardly been studied. The Upper Rhone confluences are formed by small steep tributaries (maximum and average tributary slopes of 4.0% and 1.1% respectively). During channel-forming events (*Q2*), sediments are predominantly supplied by the tributary, and consist of poorly-sorted gravels with high gradation coefficient. In addition, discharge ratios ($Qr=Q_t/Q_m$) and momentum flux ratios ($Mr=\rho Q_t U_t/\rho Q_m U_m$), two of the main controlling morphological parameters are relatively low ($0.01<Qr<0.32$ and $0.01<Mr<0.45$ respectively).

Recently, Leite Ribeiro et al. (2009) investigated this type of confluences through systematic laboratory experiments of a 90º confluence. Results revealed that the morphology of the confluence zone developed in response to these conditions is characterized by a pronounced bed discordance between the tributary and main channel, a large deposition zone in the post-confluence channel downstream of the confluence and absence of a marked scour zone. The main hydro-morpho-sedimentary processes have been assembled in a conceptual model proposed by Leite Ribeiro (2011), which contributes to the formulation of a general process-response model in extending the investigated parameter space of the foregoing studies on confluence morphodynamics (Best, 1988; Boyer et al., 2006; Rhoads et al., 2009).

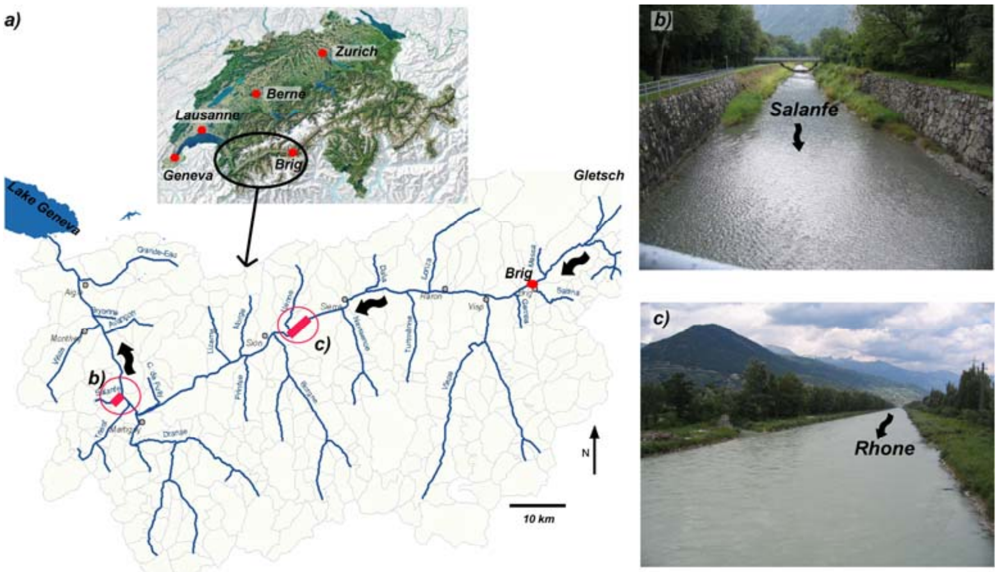

	Angle [°]	B_t/B_m	$B_m/B_{p\text{-}c}$	Tributary bed slope	Qr_Q2	Fr_{tQ2}	Mr_Q2
Average	62	0.22	1.02	1.1%	0.10	0.83	0.11
Max	90	0.54	1.27	4.0%	0.32	1.29	0.45
Min	30	0.07	0.71	0.0%	0.01	0.03	0.01

Qr_Q2= Discharge ratio between the tributary (Qt) and main channel (Qm) during a 2-year return period flood event

Fr_{tQ2} = Tributary Froude Number during a 2-year return period flood event

Mr_Q2= Momentum flux ratio between the tributary and main channel during a 2-year return period flood event

Figure 1: Upper Rhone River basin in Switzerland (a), pictures of the channelized Salanfe tributary (b) and of a typical reach of the regulated Rhone river and a table summarizing the main hydraulic and geometric characteristics of the Upper Rhone confluences.

Systematic experimental investigations of three discharge scenarios and three confluence configurations (Leite Ribeiro et al., 2011, this issue) have demonstrated that the local tributary widening in regulated confluence zones can be an excellent solution for recovering the lateral connectivity of fluvial systems. It is mainly due to the increase of the variability of flow depths, flow velocities and bed granulometry, which is favourable for the in-stream habitat and for the creation of local hotspots for biodiversity (Rohde et al., 2005; Weber et al., 2009). Furthermore, local tributary widening has no adverse impacts on flood protection.

The objective of the present paper is to investigate in detail the changes in the hydro-morpho-sedimentary processes occurring in confluence zone due to a local tributary widening. It compares its morphology and the tree-dimensional flow velocity patters with a non-widened reference configuration.

2. EXPERIMENTAL INVESTIGATION

For the present research, the designed experimental set-up is not a scale model of a particular confluence, but a schematized configuration with main geometric parameters representative of the Upper Rhone basin. The aim is to reproduce the dominant hydro-morpho-sedimentary processes occurring in this type of confluences and not to perform a case study.

The confluence flume with smooth vertical banks is composed by a 8.5 m long and 0.50 m wide main channel and a 4.9 m long and 0.15 m wide tributary, connected with an angle of 90° at a distance of 3.60 m downstream of the inlet of the main channel (Figure 2). The ratios of the tributary width to the main channel width of B_t/B_m = 0.3 and of the main channel width to the post-confluence channel width of $B_m/B_{p\text{-}c}$ = 1 are typical of river channel confluences in the Upper Rhone River **(**Figure 1). The choice of 90° confluence angle is based on the fact that the lateral valleys of the basin are almost perpendicular. The present state of the Rhone confluences zones is the result of the past river training works. Consequently the current angles are not truly natural.

Two different geometry configurations are analyzed in this paper. For the so-called reference case, the width of the tributary (B_t) is constant within the entire reach. For the so-called widened case, the width of the tributary was symmetrically doubled (B_w = 0.30 m) in the confluence zone, over a distance of

0.45 m from the tributary channel mouth (L_w=3*B_t = 0.45 m). For both reference and widened test, steady flow discharges of Q_m = 18 l/s in the main channel and Q_t = 2 l/s in the tributary were adopted (Q_t/Q_m = 0.11). Water discharges were supplied by two independent pumps, connected upstream of the main channel and the tributary. An adjustable tailgate at the end of the main channel fixed the downstream flow depth at 0.07 m.

Poorly-sorted sediments with d_{50} = 0.82 mm, d_m = 2.3 mm and d_{90} = 5.7 mm (Figure 2) were chosen for the bed material and the sediment supply. Sediments were only introduced in the tributary in a constant rate of Qs_t = 0.30 kg min^{-1} and there is no sediment transport in the main channel upstream of the confluence. This procedure aims at reproducing the typical situation of the regulated piedmont confluences during tributary flood events where the amount of the tributary solid discharge is relatively more important than that of the main channel. Sediments are supplied by a conveyor belt installed at the entrance of the tributary channel.

For each test, a systematic procedure was followed. Before each experiment, a movable bed composed by the sediment material described above was put in place. The main and post-confluence channel beds were horizontal. A step of 0.03 m is placed at the mouth of the tributary and the initial bed slope of the tributary is around 0.5%. The step and the slope are lower than the expected bed discordance and the theoretical slope.

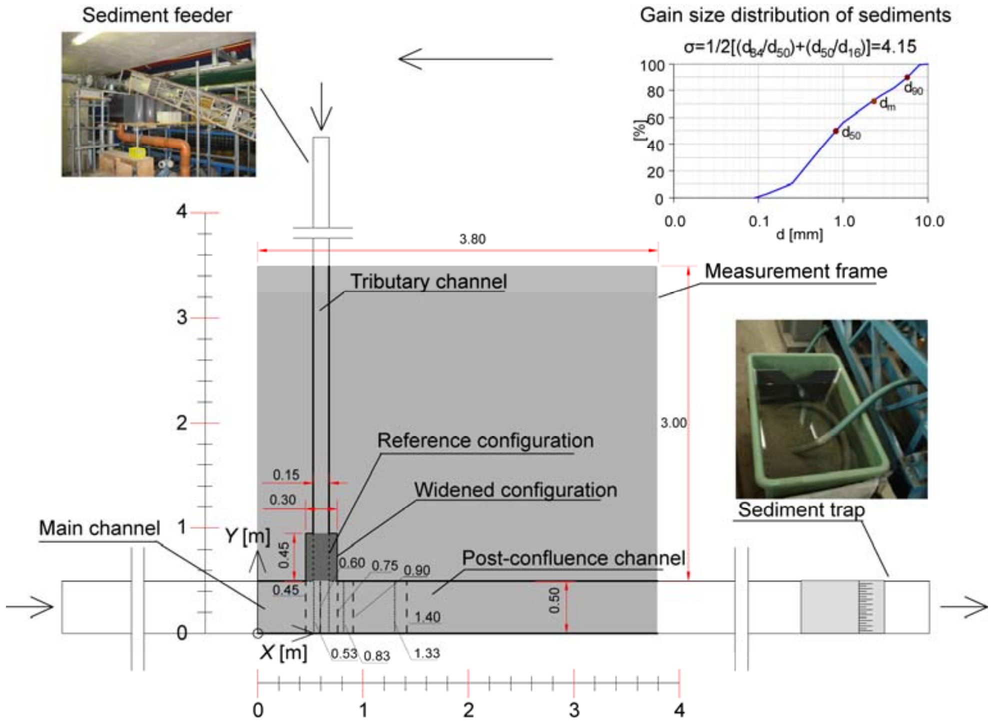

Figure 2: Experimental set-up and grain size distribution of the adopted sediment. Cross-sections where velocity measurements were performed are indicated by the dashed lines (widened configuration) and dotted lines (reference configuration).

Several campaigns of topographic surveys are performed during a run. Bed elevations are measured using a Mini EchoSounder probe (UltraLab UWS) (Kantoush et al., 2008). Each experiment was conducted until the equilibrium conditions were reached. The achievement of equilibrium in each run is mainly assessed on the basis of the bed evolution between two times steps and took 23 hours for the reference case and 22 hours for the widened case.

Once the equilibrium bed morphology was established, water surface elevations were measured with echo sounders during 10 s with a frequency of 128 Hz, providing average values. Additionally, non-intrusive measurements of velocity profiles were made with an Acoustic Doppler Velocity Profiler (ADVP), developed at the Ecole Polytechnique Fédérale de Lausanne, in Switzerland (Hurther & Lemmin, 1998). Blanckaert (2010) describes in detail the data treatment procedures and quantified the uncertainty in the measurement as follows: about 4% in the time-averaged longitudinal velocity u_x and about 10 % in the cross-stream velocities (u_y,u_z).

Three-dimensional flow velocities were measured in five cross-sections in the main and post-confluence channels: i.e, at the upstream corner of the confluence ($X = 0.53$ m in the reference configuration and $X = 0.45$ m in the widened configuration), at the axis of the tributary ($X = 0.60$ m), at the downstream corner of the confluence ($X = 0.68$ m in the reference configuration and $X = 0.75$ m in the widened configuration), and distances of 0.15 m and 0.65 m downstream of the confluence.

3. BED MORPHOLOGY AND WATER LEVELS

For both tests, the main equilibrium morphological features (Figure 3) are similar to those presented in Leite Ribeiro et al. (2009), i.e, pronounced bed discordance between the tributary and the main channel; presence of a large sediment deposition bar downstream of the confluence at the inner bank; and small erosion near the outer bank.

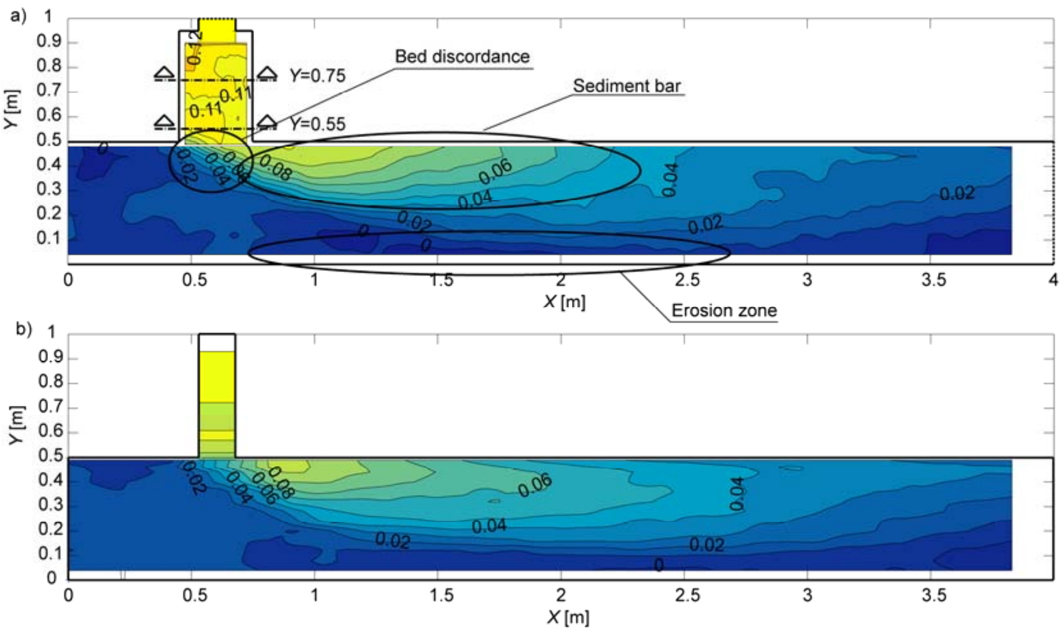

Figure 3: Equilibrium bed morphology of the main, post-confluence and part of the tributary channel for the widened (a) and the reference configurations (b).

Water surface elevations in the widening zone are equal to those in the reference configuration. However, there is a considerable overall rise in bed elevation in the local tributary widening compared to the reference configuration (Figure 4). Therefore for the widened configuration, the flow depth in the axis is reduced to 0.01 m, which corresponds to half of the average flow depth in the reference tributary (0.02 m), whereas the maximum flow depth in the thalweg of 0.018 m is still smaller than the reference flow depth in the tributary. The local widening of the tributary leads to a reduction of about 15% in effective cross-sectional flow area measured at $Y = 0.55$ m as compared to the reference configuration. This leads to an increase of the tributary velocities provided to the main channel, which can be expected to enhance the morphodynamic processes in the confluence zone. Despite the bed elevation rise in the widened zone, the local widening does not influence the water and bed elevations of the tributary upstream of the widened zone.

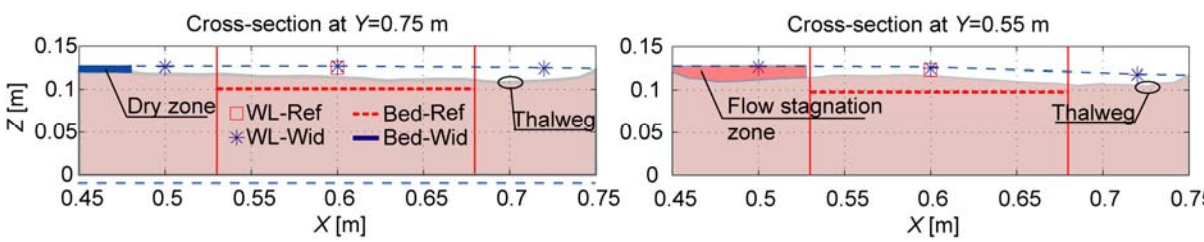

Figure 4: Cross-sections situated in the middle of the local tributary widening (*Y*=0.75 m) and near the tributary mouth (*Y*=0.55 m).

The local tributary widening promotes an increase of the bed discordance and of the tributary penetration, which resulted in a general rise of the bed level in the confluence zone (Figure 5). As illustrated by Figure 6, the general bed rise can be recognized by the formation of a dry zone near the inner bank downstream of the confluence, which is not observed for the reference case. The influence of the local tributary widening however is only limited to the confluence zone. For $X > 1$ m, the cross-sectional averaged bed levels are identical (Figure 5). This could have been expected, since the total flow and sediment discharge in the post-confluence channel are not modified by the local tributary widening. It is also important to notice that the average increase of bed elevations at the confluence zone does not affect the upstream water elevations in the main channel (Figure 5).

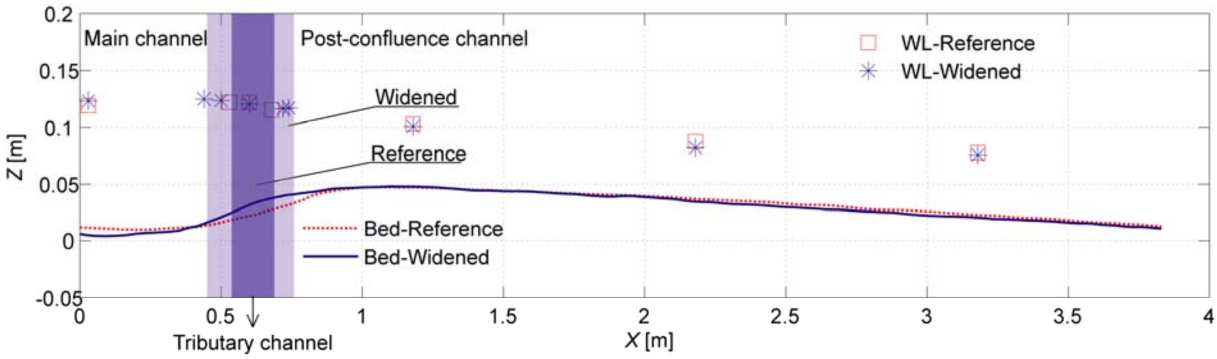

Figure 5: Cross-sectional averaged water and bed elevations in the main and post-confluence channels.

4. FLOW DYNAMICS

4.1. Flow visualization

Flow expands upon entering the local tributary widening (Figure 6a). The influence of the flow in the main channel induces an asymmetry of the flow expansion, which is deviated towards the inner (downstream) bank of the widened zone. The tributary flow is reattached to the inner bank. The flow deviation, however, does not allow the flow to reattach to the outer bank. As a result of this deviation, the tributary flow enters the main channel with an angle of 65° (Figure 6a).

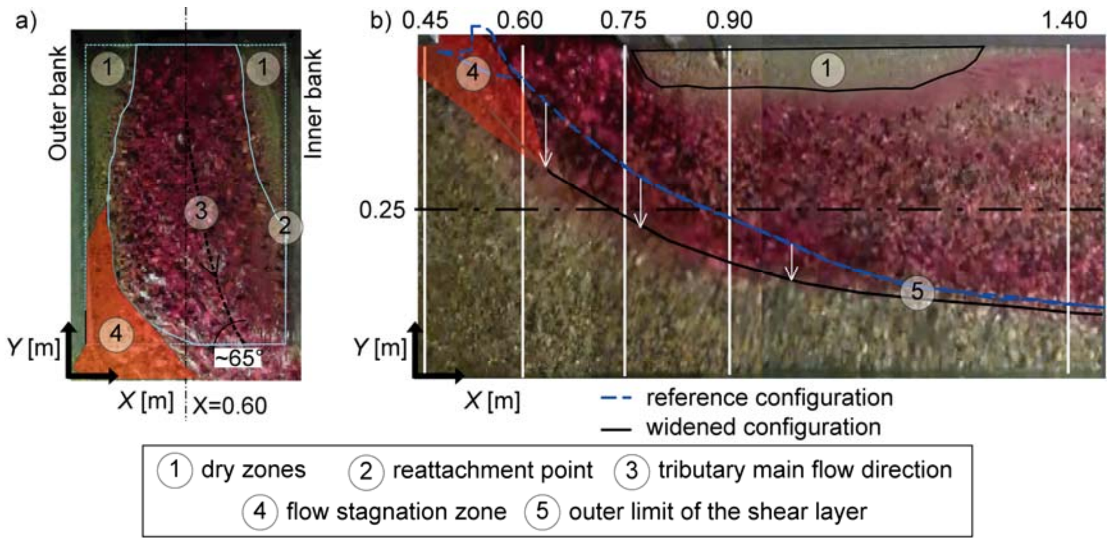

Figure 6: Flow visualisation of the widened configuration. a) Local tributary widening and b) main and post-confluence channels. The location of the outer limit of the shear layers at the water surface is indicated by the full black line. For comparison matter, the outer limit of the shear layer for the reference case is shown by the dashed blue line. The coordinate axes are not placed at the origin.

4.2. Depth-averaged flow field

Figure 7 assesses the influence of the local tributary widening on the bed morphology and the normalized streamwise unit discharge ($U_x h/UH$) by comparison of corresponding cross-sections in the reference configuration and the configuration with local tributary widening.

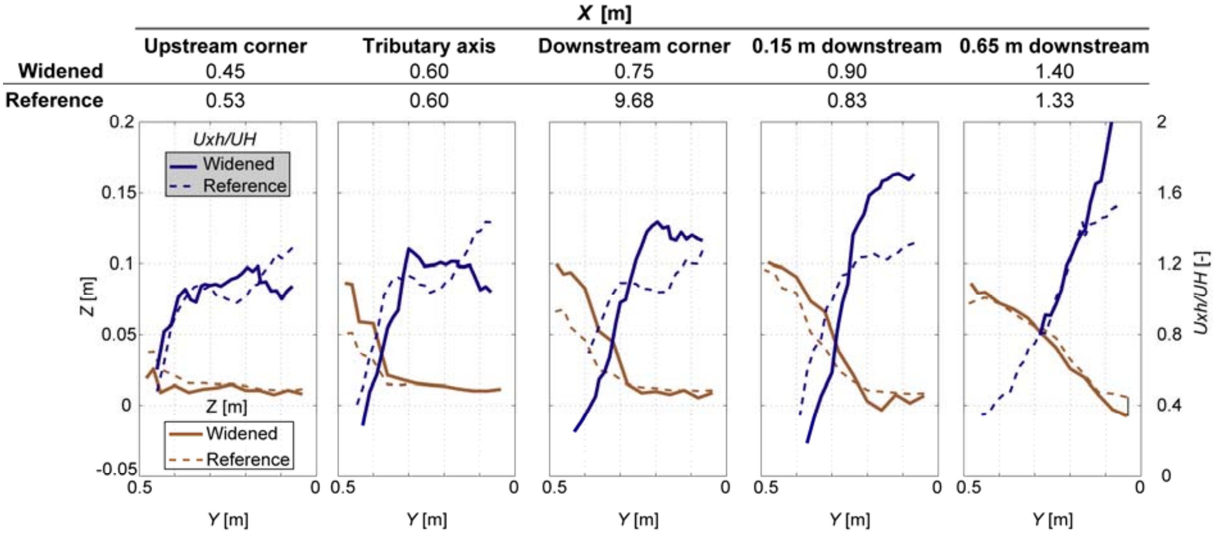

Figure 7 Comparison of the normalized stremwise unit discharge (*$U_x h/UH$*) and the bed morphology in the reference configuration (dashed lines) and in the configuration with local tributary widening (full lines). a) At the upstream confluence corner; b) at the tributary axis, c) at the downstream confluence corner, d) 0.15 m downstream of the confluence, e) 0.65 m downstream of the confluence. U_x denote the local streamwise depth-averaged velocity, h the local flow depth, U the average cross-sectional streamwise velocitiy and H the mean cross-sectional flow depth.

The bed morphology and the $U_x h/UH$ in the cross-section at the upstream corners of the confluences (X = 0.53 m for the reference configuration and X = 0.45 m for the widened test) are rather similar. The normalized streamwise unit discharges are already slightly outwards skewed. This can be attributed to topographic steering due to the presence of the bar just downstream as well as to the obstruction by the inflow originating from the tributary. The local tributary widening has a marked influence on the bed morphology and on $U_x h/UH$ from the cross-section located at the tributary axis. Bed elevations are higher for the widened case due to the higher bed discordance and the increased tributary penetration into the post-confluence. This leads to reduced normalized streamwise unit discharges in the inner part of the cross-section. Outwards deflection of the flow increases the unit discharge in the outer part of the cross-section. In the reference configuration, the maximum value of $U_x h/UH$ is found at the outer bank. In the configuration with local tributary widening, the outward flow deflection has not yet reached the outer bank and the maximum $U_x h/UH$ is found in the central part of the cross-section. In the cross-section located at the downstream corner of the confluence, the local tributary widening causes a global decrease/increase of the unit discharge in the inner/outer part of the cross-section. The occurrence of a dry zone at the inner bank in the configuration with local tributary widening considerably affects the distribution of $U_x h/UH$ in the cross-section situated 0.15 m downstream of the confluence. It amplifies the decrease/increase of the $U_x h/UH$ in the inner/outer part of the cross-section and leads to an increased $U_x h/UH$ at the outer bank. Morphological differences between both configurations have about died out in the cross-section 0.65 m downstream of the confluence, which corresponds to the downstream limit of the dry zone in the configuration with local tributary widening. The normalized streamwise unit discharge at the outer bank is still considerably higher, however, in the configuration with local tributary widening. Due to the increased erosion (maximum about 0.015 m or about 15% of the flow depth) and the increased $U_x h/UH$ near the outer bank, the local tributary widening may increase the flow attack on the outer bank.

4.3. Three-dimensional flow field

The amplification of the hydrodynamic processes in the confluence induced by the local tributary widening are well illustrated in Figure 8, which compares the near bed (Z/h = 0.2) and near-surface (Z/h = 0.7) velocities in both configurations. Near the inner bank, the near-bed flow from the main channel follows a rather straight path and it is directed upslope the bar (most left near-bed vectors in X = 0.45 m and X = 0.60 m in the widened configuration and in X = 0.53 m and X = 0.60 m in the reference configuration). The dominant tributary inflow (in X = 0.75 m in the widened configuration and in X = 0.60 m in the reference configuration) can easily be recognized by the near surface velocities that are outwards directed. Their skewing with respect to the near-bed velocities illustrates the two-layer flow structure, which mainly occurs in the region confined by the shear layer.

The presence of the stagnation zone where the tributary and main-channel flows collide is clearly discernable in the low near surface velocities, occurring near the tributary axis in the widened configuration and near the upstream confluence corner in the reference configuration (Figure 8).

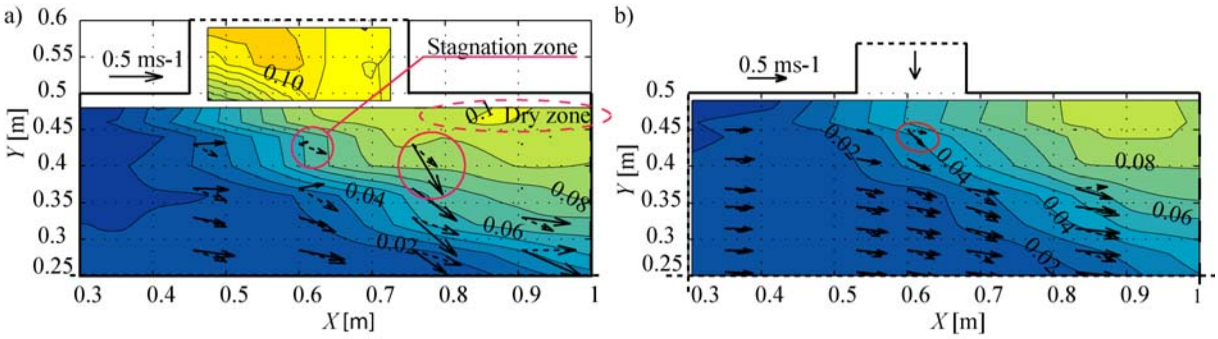

Figure 8 Velocity vectors (u_x,u_y) near the bed at Z/h=0.2 (dashed vectors) and near the surface at Z/h=0.70 (full vectors) superimposed on the local bed morphology. (a) Configuration with local tributary widening, (b) reference configuration. The dashed circle in (a) indicates approximately the dry zone.

5. CONCLUSIONS

Laboratory experiments indicate that local tributary widening considerably affects the hydro-morpho-sedimentary processes in the confluence zone. Although the local tributary widening allows a realignment of the tributary flow and a corresponding reduction in the confluence angle, it leads to an amplification of the morphodynamic processes in the confluence zone. This somewhat counterintuitive result is due to the reduction of the effective flow area in the local tributary widening and the corresponding increase in the tributary velocities and the tributary momentum flux. The reduction in effective flow area allows satisfying the requirements of sediment transport continuity in the local tributary widening. It occurs by means of a general rise in the bed elevation and by a lateral constriction of the flow induced by a zone of flow stagnation at the upstream confluence corner.

The increased tributary velocities accentuate and amplify the two-layer flow structure in the confluence zone. Flow originating from the tributary remains in the upper part of the water column and is strongly outwards directed. Flow originating from the main channel remains in the lower part of the water column and is less outwards directed.

The increased tributary momentum flux due to the local tributary widening leads to an increased bed discordance and a deeper tributary penetration in the confluence zone for the studied discharge scenario. Downstream of the confluence zone, increased deposition/erosion in the inner/outer part of the cross-section amplifies the bed morphology gradients. This represents mainly morphological redistribution, however, because the cross-sectional flow area and the water surface elevations remain unchanged. This morphological redistribution amplifies the topographic steering of the flow and the corresponding transverse fluxes of mass and momentum.

6. ACKNOWLEDGMENTS

The research is supported by the Swiss Federal Office for the Environment (FOEN) in the framework of the research project “Integrated management of river systems”.

7. REFERENCES

Best, J. L. (1987). *Flow dynamics at river channel confluences: Implications for sediment transport and bed morphology*. Recent Developments in Fluvial Sedimentology, Spec. Publ. SEPM Soc Sediment Geol, 39(Spec. Publ. SEPM Soc. Sediment. Geol.), pp.27-35.

Best, J. L. (1988). *Sediment transport and bed morphology at river channel confluences*. Sedimentology, 35(3), pp.481-498.

Biron, P., Roy, A. G. and Best, J. L. (1996). *Turbulent flow structure at concordant and discordant open-channel confluences*. Experiments in Fluids, 21(6), pp.437-446.

Biron, P., Roy, A. G., Best, J. L. and Boyer, C. J. (1993). *Bed morphology and sedimentology at the confluence of unequal depth channels*. Geomorphology, 8(2-3), pp.115-129.

Blanckaert, K. (2010). *Topographic steering, flow recirculation, velocity redistribution, and bed topography in sharp meander bends*. Water Resour. Res., 46(9), pp.W09506.

Bourgeois, M. 2006. *Accroissement de la valeur naturelle de la vallée du Rhône par un raccordement optimal des affluents du Rhône*, LCH-EPFL**:** 152.

Boyer, C., Roy, A. G. and Best, J. L. (2006). *Dynamics of a river channel confluence with discordant beds: Flow turbulence, bed load sediment transport, and bed morphology*. Journal of Geophysical Research, 111(F04007), pp.1-22.

Hurther, D. and Lemmin, U. (1998). *A constant-beam-width transducer for 3D acoustic Doppler profile measurements in open-channel flows*. Measurement Science & Technology, 9(10), pp.1706-1714.

Kantoush, S. A., De Cesare, G., Boillat, J. L. and Schleiss, A. J. (2008). *Flow field investigation in a rectangular shallow reservoir using UVP, LSPIV and numerical modelling*. Flow Measurement and Instrumentation, 19(3-4), pp.139-144.

Leite Ribeiro, M. 2011. *Influence of Tributary Widening on Confluence Morphodynamics*. Laboratory of Hydraulic Constructions (LCH). Lausanne, Ecole Polytechnique Fédérale de Lausanne. PhD.

Leite Ribeiro, M., Blanckaert, K., Boillat, J. L. and Schleiss, A. J., 2009. Influence of the momentum flux ratio on confluence morphology. 3rd IAHR Congress "Water Engineering for a Sustainable Environment", Vancouver, Canada.

Leite Ribeiro, M., Blanckaert, K. and Schleiss, A. J., 2011. Influence of tributary widening on the morphology and the hydraulic variability in confluence zones. 34th IAHR World Congress, Brisbane, Australia.

Rhoads, B. L. and Kenworthy, S. T. (1995). *Flow structure at an asymmetrical stream confluence*. Geomorphology, 11(4), pp.273-293.

Rhoads, B. L., Riley, J. D. and Mayer, D. R. (2009). *Response of bed morphology and bed material texture to hydrological conditions at an asymmetrical stream confluence*. Geomorphology, 109(3-4), pp.161-173.

Rohde, S., Schutz, M., Kienast, F. and Englmaier, P. (2005). *River widening: An approach to restoring riparian habitats and plant species*. River Research and Applications, 21(10), pp.1075-1094.

Weber, C., Schager, E. and Peter, A. (2009). Habitat diversity and fish assemblage structure in local river widenings: A case study on a Swiss River. River Research and Applications, 25(6), pp.687-701.